

Numerical Simulation of Nano-disk Plasmonic Laser

Qian Wang¹⁾ and Seng-Tiong Ho^{1,2)}

1) Data Storage Institute, Agency for Science, Technology and Research

2) Dept. Electrical Engineering and Computer Science, Northwestern University, Evanston, IL, 60208
(wang_qian@dsi.a-star.edu.sg)

Abstract-Numerical simulation of a nano-disk based plasmonic laser is presented. A semiconductor nano-disk embedded in the gold forms a cavity for the plasmonic laser. One-dimensional body-of-revolution finite-difference-time-domain incorporated with Drude model for the metal and multilevel/multi-electron gain medium model is developed for the simulation. The lasing performance of the nanodisk with a radius of 90 nm is numerically demonstrated.

Index Terms-plasmonic laser, nanodisk, simulation

I. INTRODUCTION

Nano-plasmonic integration circuits can further scale down the footprint of photonic device compared to current high-index contrast waveguide devices. A nanoplasmonic laser filled with semiconductor gain medium can be an integrated light emitter for the nanoplasmonic integration[1]. In this paper, a nanoplasmonic laser based on semiconductor nano-disk embedded in the gold as shown in Fig. 1a is designed and numerically simulated.

Due to the axial symmetric feature of the laser cavity, we developed a fast simulation approach with body-of-revolution finite-difference-time-domain incorporating with the Drude model for the metal and multi-level/multi-electron model for the gain medium[2,3]. This simulation approach can provide a temporal and spatial electromagnetic simulation of the lasing performance. Design and simulation of this nanoplasmonic laser includes three-steps as shown in the paper: 1) using a BOR-FDTD to find out the spectrum response of the “cold” laser cavity, which gives the resonant wavelength corresponding to a given disk radius; 2) using BOR-FDTD with gain medium model and also appropriate gain medium parameters, e.g., the band-gap wavelength, the lasing performance of the nanodisk is simulated under different pumping condition; and 3) the recorded field in the time-domain is analyzed which gives the lasing spectrum and the relationship between injection current density and emitting power of the laser. As an example, a semiconductor nanodisk plasmonic laser with a radius of 90 nm is numerically demonstrated of which the lasing wavelength is 1470nm.

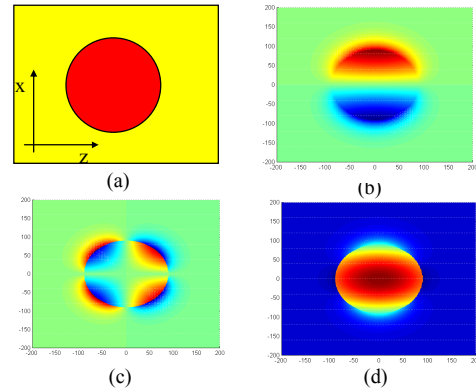


Fig.1 (a) schematic structure of the nano-disk laser; (b-d) eigenmode of the lasing cavity; (b) Hy; (c) Ex; (d) Ez.

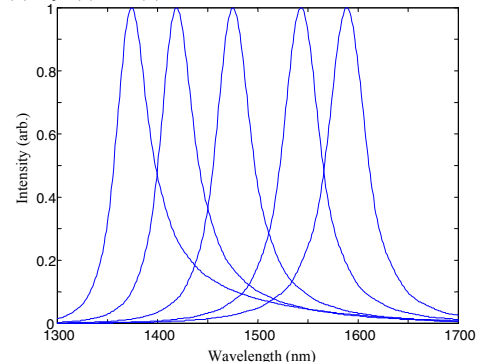


Fig.2 Spectrum response of the nanoplasmonic cavity for radius from 80 nm to 100 nm with an incremental step of 5nm.

II. SIMULATION OF THE NANOPLASMONIC LASER

Body-of-revolution finite-difference-time-domain can reduce the simulation time/resource requirement significantly through using the axial symmetric of the structure. In this paper, it is incorporated with Drude modal for the metal and multilevel multielectron modal for the semiconductor gain medium for this nanodisk plasmonic laser.

The Maxwell equation with body of revolution in the cylinder coordinate is

$$\begin{cases} \frac{\partial H_z}{\partial t} = -\frac{1}{\mu} \left(\frac{1}{r} \frac{\partial (rE_\phi)}{\partial r} + \frac{1}{r} mE_r \right) \\ \frac{\partial D_r}{\partial t} = \left(\frac{1}{r} mH_z \right) \\ \left(\frac{\partial D_\phi}{\partial t} \right) = \left(-\frac{\partial}{\partial r} H_z \right) \end{cases} \quad (1)$$

The Drude model for metal is included in the Maxwell equation through the polarization $\frac{\partial D_i}{\partial t} = \epsilon \frac{\partial E_i}{\partial t} + \sum_{m=1}^M \frac{\partial P_{mi}}{\partial t}$ ($i=r, \phi$, and $M=1, \epsilon = \epsilon_\infty$). For the Drude model of metal, the update of the

polarization is $\frac{\partial^2 P_i}{\partial t^2} + \Gamma \frac{\partial P_i}{\partial t} = \epsilon_0 \omega_p^2 E_i$. With the cold cavity (without carriers), the eigenmode profile of the nano-cavity calculated using this BOR-FDTD is shown in Fig.1(b), Fig.1(c) and Fig.1(d) for H_y , E_x and E_z , respectively. The spectrum response of the nanodisk cavity is given in Fig.2 for a disk radius ranging from 80 nm to 100 nm with an incremental of 5 nm (the refractive index of the semiconductor is 3.5). In our nanoplasmonic laser simulation, the nanodisk with a radius of 90 nm is chosen a numerical example in the below simulation.

For the active cavity with gain medium, the multilevel and multi-electron model updates the polarization through

$$\frac{d^2 \vec{P}_m}{dt^2} + \gamma_m \frac{d \vec{P}_m}{dt} + \left(\omega_m^2 + \frac{2\omega_m^2 |\vec{\mu}_m|^2}{\hbar^2} |\vec{A}|^2 \right) \vec{P}_m = 2 \frac{\omega_m |\vec{\mu}_m|^2}{\hbar} \vec{E} (N_{C_m} - N_{V_m}) \quad (2)$$

and the corresponding rate equations

$$\frac{dN_{C_m}(t)}{dt} = -\frac{\omega_m}{\hbar} \vec{A}(t) \cdot \vec{P}_m - \frac{N_{C_m}(t) \left(1 - \frac{N_{V_m}(t)}{N_{V_m}} \right)}{\tau_m} - \frac{N_{C_m}(t) \left(1 - \frac{N_{C_{m-1}}(t)}{N_{C_{m-1}}} \right)}{\tau_{m,m-1}} \quad (3a)$$

$$+ \frac{N_{C_{m+1}}(t) \left(1 - \frac{N_{C_m}(t)}{N_{C_m}} \right)}{\tau_{m+1,m}} + W_p$$

$$\frac{dN_{V_m}(t)}{dt} = \frac{\omega_m}{\hbar} \vec{A} \cdot \vec{P}_m + \frac{N_{C_m}(t) \left(1 - \frac{N_{V_m}(t)}{N_{V_m}} \right)}{\tau_m} - \frac{N_{V_m}(t) \left(1 - \frac{N_{V_{m-1}}(t)}{N_{V_{m-1}}} \right)}{\tau_{m,m-1}} \quad (3b)$$

$$+ \frac{N_{V_{m+1}}(t) \left(1 - \frac{N_{V_m}(t)}{N_{V_m}} \right)}{\tau_{m+1,m}} - W_p$$

Detailed definitions of the gain medium parameters and their typical values can be found in Ref.[3] With this gain medium model, lasing performance of the nano-disk is simulate under different injection current density which determines the pumping power $W_p = eJ/d$. Using $J=800 \text{ A/cm}^2$ as example, the detected field (detector is put at $r=45 \text{ nm}$) in the time-domain is shown in Fig.3a and with spectrum analysis of this result, the corresponding lasing wavelength is shown in Fig.3b. Compared to the spectrum response of the cold cavity, the lasing wavelength has a slight shift which is caused by the change of the refractive due to injection of the carriers.

With different injection current density, the I-L curve is simulated for this nanoplasmonic laser and corresponding relationship is shown in Fig.4, which shows the threshold value of $\sim 580 \text{ A/cm}^2$ for this nanoplasmonic laser.

III. CONCLUSION

A nanoplasmonic laser with semiconductor gain is simulated and designed. The body of revolution finite-difference-time-domain incorporated with the

Drude-modal for the metal and multilevel and multi-electron model for the gain medium is developed for this numerical simulation. The lasing performance of this nanodisk plasmonic laser with a radius of 90 nm is numerically demonstrated.

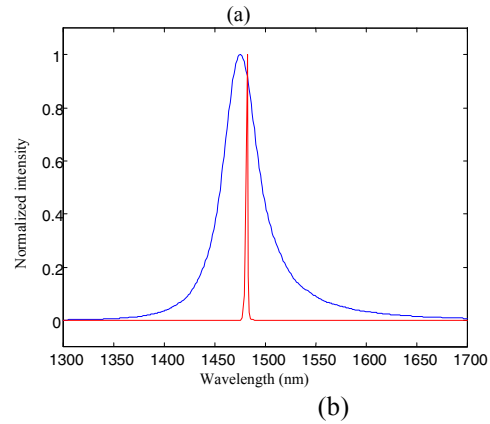
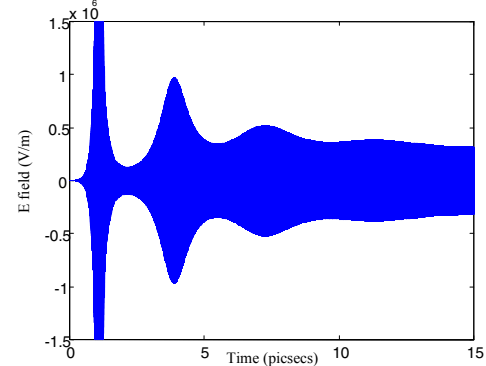


Fig.3 a) Electric field recorded in the time-domain; b) lasing wavelength of the nanoplasmonic laser.

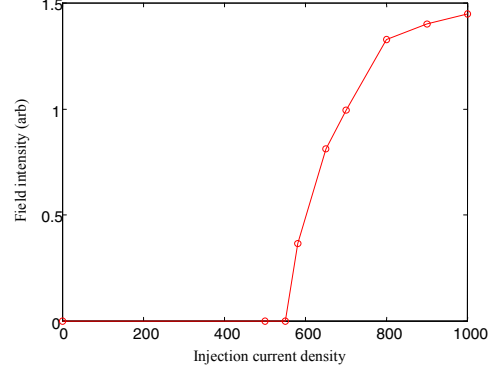


Fig.4 I-L curve simulated for this nanoplasmonic laser.

REFERENCE

- [1] M.T. Hill, M. Marell, E. S. P. Leong et.al, "Lasing in metal-insulator-metal sub-wavelength plasmonic waveguides", Opt. Expr., Vol.17, No.13, pp.11107-11112, 2009.
- [2] D. B. Davidson, "Body-of-revolution finite-difference time-domain modeling of space-time focusing by a three-dimensional lens", J. Opt. Soc. Am, A vol.11, No.4, pp. 1471-1490.
- [3] Y. Huang and S. T. Ho, "Computational model of solid-state, molecular, or atomic media for FDTD simulation based on a multi-level multi-electron system governed by Pauli exclusion and Fermi-Dirac thermalization with application to semiconductor photonics", Opt. Expr., Vol14, No.8, 2006, pp. 3569-3587.